In vitro and in vivo Evaluation of Chemically Synthesized, Receptor-Biased Interleukin-4 and Photocaged Variants

Mamiko Ninomiya[1], Cecilie Egholm[2], Daniel Breu[2], Onur Boyman*[2,3], and Jeffrey W. Bode*[1]

[1]Department of Chemistry and Applied Biosciences, ETH Zurich, 8093 Zurich, Switzerland.
[2]Department of Immunology, University of Zurich, University Hospital Zurich, 8091 Zurich, Switzerland.
[3]Faculty of Medicine and Faculty of Science, University of Zurich, 8006 Zurich, Switzerland

Abstract

Interleukin-4 (IL-4) is a cytokine that plays a central role in type 2 immune responses and is involved in regulating pleiotropic actions in our body by engaging multiple different IL-4 receptor (IL-4R) complexes. Targeting the IL-4R system has a high potential for therapeutic intervention for allergic and autoimmune diseases. A challenge in developing this pleiotropic cytokine for clinical application is the construction of variants tailored for engagement with specific receptor IL-4R subunits, which are necessary for selective activation of specific signaling pathways to treat disease with minimum side effects. To establish a platform for preparation of tailored IL-4 variants, we developed a modular and flexible chemical synthesis of IL-4 and applied this approach to the preparation of (i) IL-4 variants that act as receptor antagonist due to presence of unnatural residues that block specific interactions, and (ii) photocaged and in vivo half-life extended IL-4 variants that can be conditionally activated using UV light, achieved by the incorporation of a photocaged Gln116 residue. We were able to show that these different cytokine variants elicit differential STAT5 or STAT6 phosphorylation in lymphocytes or neutrophils in vitro with just one amino acid substitution. Furthermore, we demonstrated that the photocaged IL-4 can be activated by UV light and effectively suppresses neutrophils in an inflammation model in vivo. Collectively, this work demonstrated the flexibility and applicability of chemical protein synthesis by allowing us to broaden the scope of protein variants that can be accessed for the preparation and evaluation of therapeutically valuable proteins.

Introduction

Cytokines are a large class of small proteins that contribute to diverse cellular functions and cellular fates. Given their importance in inflammation and immune reactions, cytokines have been approved and used in the context of cancer immunotherapy since the 1980s.[1] Despite their clinical potential and early successes, the further development of cytokine therapies is hampered by their short half-life, requiring multiple administrations that in combination with their pleiotropic nature leads to severe side effects. Strategies to specifically tailor functions and properties of cytokines to harness their full therapeutic potential are required.[2] Recently, owing to the better understanding of cytokine immunobiology and structural biology, advances have been made by recombinant protein engineering to produce activity-modulated cytokines including muteins, conditionally activatable cytokines, superkines, computationally designed neoleukins, and orthogonal cytokine-receptor pairs.[3–6]

Interleukin-4 (IL-4) is a classical four-α-helical bundle cytokine that plays a central role in type 2 immune responses. IL-4 is involved in different immune processes, including differentiation of naive T cells to T helper 2 (Th2) cells, immunoglobulin (Ig) class switching to IgE, dendritic cell maturation, and macrophage activation.[4] IL-4 confers its pleiotropic actions by engaging two types of heterodimeric IL-4 receptor (IL-4R) complexes on cell surfaces. The type I IL-4R is comprised of IL-4Rα and γc,

while type II IL-4R is formed by IL-4Rα and IL-13Rα1 (Fig. 1). In both IL-4R complexes, IL-4 primarily binds to IL-4Rα with high affinity (K_D = ~10^{-10} M), after which IL-4–IL-4Rα recruits the low-affinity receptor subunit, either γc or IL-13Rα1 (K_D = ~10^{-6} M).[7] Type II IL-4R can also be bound by IL-13, which rationalizes the observation that IL-4 and IL-13 have overlapping biological activities in certain cell types. After forming heterodimeric complexes, both type I and II IL-4Rs activate the intracellular JAK-STAT signaling pathway by phosphorylating JAK1, JAK3, TYK2, STAT5 and/or STAT6), after which phosphorylated STAT (pSTAT) dimers translocate into the nucleus. While IL-4Rα is expressed widely over different cell types, the expression of the second low-affinity receptor subunits γc and IL-13Rα1 is highly dependent on the cell types. γc is mainly expressed in hematopoietic cells, such as T and B cells, whereas IL-13Rα1 is expressed in non-hematopoietic cells and some myeloid cells.[7–12]

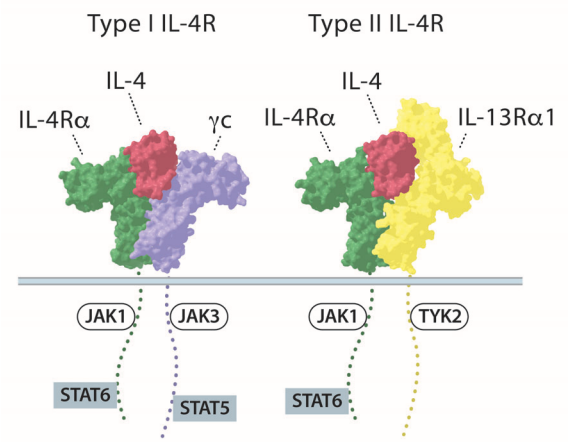

Figure 1. IL-4 receptor system. Type I IL-4R consists of IL-4Rα and γc, and type II IL-4R consists of IL-4Rα and IL-13Rα1.

Despite its important role in type 2 immune responses, dysregulated IL-4 is implicated in the pathogenesis of allergic diseases, which affect large parts of the global population. Since IL-4 signaling is involved in the essential steps of the development and evolution of allergic diseases, blocking IL-4 signaling is regarded as an ideal target for the prevention and treatment of allergic diseases.[9,13] Previously, efforts have been made to engineer IL-4 mutants as well as IL-4 conjugates that act as an antagonist by preventing the binding of the second receptors.[14–16] Dupilumab, an anti-IL-4Rα monoclonal antibody, blocks IL-4R-mediated signaling and was approved for atopic dermatitis in 2017 and for asthma in 2018 by the FDA.[17–19]

While overproduction of IL-4 is an undesired element in atopic disease, IL-4 could be a treatment for certain autoimmune diseases such as psoriasis. Neutrophils are tightly involved in the development and progression of psoriasis by leading to inflammation, attracting other inflammatory immune cells, and forming neutrophil extracellular traps (NETs), which altogether lead to the destruction of healthy tissue.[20,21] Recent studies showed that IL-4R signaling in neutrophils has an inhibitory effect by curtailing neutrophil migration, phagocytosis and NET formation and by accelerating their cellular aging,[10,12,22–24] explaining the increasing interests in using engineered IL-4 variants as potential treatments for patients with neutrophilic autoimmune and autoinflammatory disease.[25,26]

In order to shepherd IL-4 function towards a specific disease area, it is advantageous to be able to tailor IL-4 on an atomic-level, in order to modulate its properties and binding affinities. Here, we describe the chemical synthesis of IL-4 using the α-ketoacid-hydroxylamine (KAHA) amide-forming ligation.[27,28] This modular synthetic route enabled us to generate IL-4 variants

that (i) block or differentiate between the two IL-4R complexes, and (ii) serve as half-life extended photocaged IL-4R agonists for spatiotemporally controlled treatment of mouse models of neutrophilic inflammation. This was achieved by using chemical protein synthesis to incorporate multiple non-canonical amino acids bearing unique functional groups, including photoactivatable amino acid and conjugation handles. Taken together, our data demonstrate the facile modulation and manipulation of bioactive molecules using a chemical synthesis platform for cytokine engineering to control receptor binding and selectivity.

Results

Synthesis of mouse IL-4 wild-type

While IL-4 is prevalent in all mammals, the sequence divergence is high among different species.[29] For example, mouse and human IL-4 have sequence identity of only 41% and do not exhibit cross-reactivity. Although most previous antagonist development studies were based on human IL-4, we decided to focus on the mouse system to facilitate in vivo studies. Mouse IL-4 consists of 120 amino acids including 6 cysteines, all of which are involved in disulfide bonds (Cys5–Cys87, Cys27–Cys67, Cys49–Cys94).[30,31] From the primary sequence, we envisioned synthesizing IL-4 from three segments using two KAHA ligations (Fig. 2a). The ligation sites were chosen to be Leu36–Thr37 and Leu75–Met76. The most convenient implementation of KAHA ligation employs 5-oxaproline as the hydroxylamine, as this building block is readily available and forms more soluble peptide esters as the primary ligation product. This building block introduces a non-canonical homoserine residue at the ligation site, and we identified the Thr37Hse and Met76Hse mutations as being unlikely to interfere with receptor interactions. Temporary acetaminomethyl (Acm) group[32] were used as orthogonal protecting groups for the cysteines to avoid oxidation and undesired disulfide scrambling during the synthesis; likewise methionine residues were replaced with norleucines to avoid oxidation.

Each peptide segment was prepared by Fmoc solid-phase peptide synthesis (SPPS). C-terminal α-ketoacid-bearing peptide segments **1** and **2** were synthesized using our established standard protocol for peptide α-ketoacids.[28] For orthogonality during the KAHA ligation, the α-ketoacid in the middle segment **2** was protected with a photolabile group. The cleavage of the peptides from the resin and purification by reverse-phase high performance liquid chromatography (RP-HPLC) gave the desired peptide segments **1** and **2** in good yield (18% and 21% yield, respectively). The synthesis of C-terminal segment **3** proved challenging due to its hydrophobicity. However, after screening multiple resins and dipeptides, the use of polyethylene glycol (PEG)-based HMPB ChemMatrix® resin and introduction of two pseudoprolines[33] at Ile92-Ser93 and Ser101-Thr102 during the synthesis afforded us the desired peptide **3**, albeit in low yield (3.3 % overall yield based on the loading of the resin), which could be due to the low solubility and chromatographic recovery.

The linear protein was assembled from the synthetic segments in a sequential manner (Fig. 2b). Segments **1** and **2** were ligated under standard KAHA ligation conditions (20 mM, 9:1 DMSO:H_2O containing 0.1 M oxalic acid, 60 °C) followed by UV irradiation to remove the α-ketoacid protecting group; the product was purified by RP-HPLC to obtain **4** in 51% yield (Fig. 2c). Peptide **4** was coupled with segment **3** by KAHA ligation using the same conditions to yield linear IL-4 containing two homoserine depsi-peptides, which is the primary product of KAHA ligations with 5-oxaproline. These ester bonds were directly rearranged to amide bonds by diluting the ligation solution with a basic buffer (50 mM sodium carbonate, 6 M Gn·HCl, pH 9.5) to give linear protein **5** in 33% yield over two steps (Fig. 2d). The Acm protecting groups were removed by the treatment with AgOAc in AcOH/water for 1 h at 50 °C, affording linear IL-4 (**6**) in 79% yield.

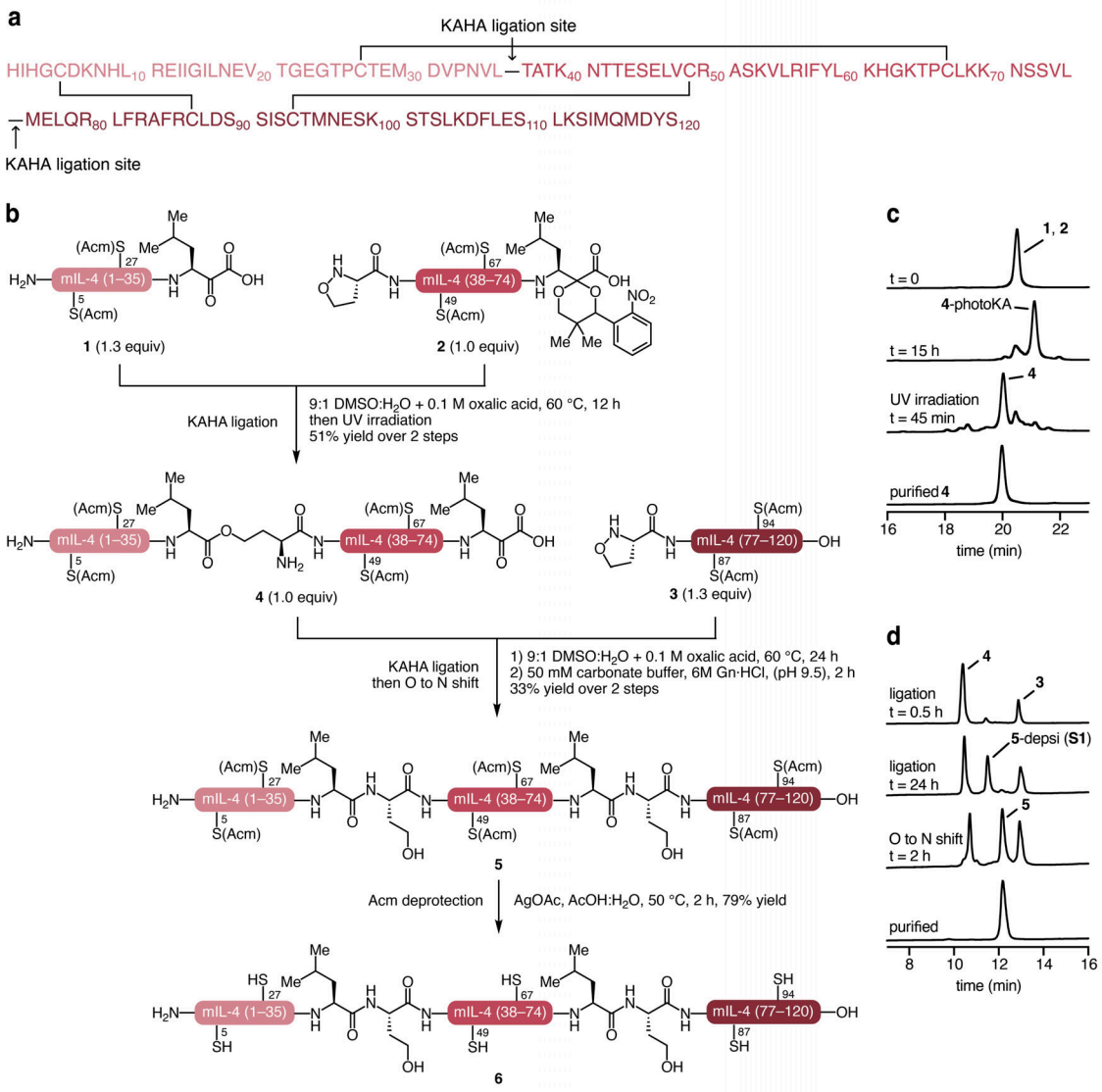

Fig. 2 a) Amino acid sequence of mouse IL-4 showing the ligation sites. b) Synthesis of linear IL-4 **6** by sequential KAHA ligations. c) Analytical HPLC monitoring of ligation between segment **1** and **2** to yield peptide **4**. d) Analytical HPLC monitoring of ligation between peptide **4** and **3** to obtain polypeptide **5**.

Initial attempts to fold **6** based on the reported conditions for recombinantly expressed mouse IL-4 did not yield sufficient quantities of the folded protein.[30] After optimization of denaturant, pH, concentration, and redox reagents, we identified suitable conditions: a lyophilized powder of **6** was dissolved in buffer A (6 M Gn·HCl, 40 mM Tris, 1 mM EDTA, pH 8.5) at a concentration of 0.5 mg/mL. The protein solution was diluted 6 times in the buffer B (0.5 M Arg·HCl, 40 mM Tris, 5 mM Cys, pH 8.5) and incubated overnight at room temperature (Fig. 3a). After acidification, the folded IL-4 **7** was successfully purified by RP-HPLC with 48% isolated yield (Fig. 3b). The mass and purity of folded synthetic IL-4 was confirmed by electrospray ionization high-resolution mass spectrometry (ESI-HRMS), sodium dodecyl sulphate polyacrylamide gel electrophoresis (SDS-PAGE), and RP-HPLC (Fig. 3b, c, d). In addition, the circular dichroism (CD) spectrum of **7** showed a distinct α-helix pattern (Fig. 3e).

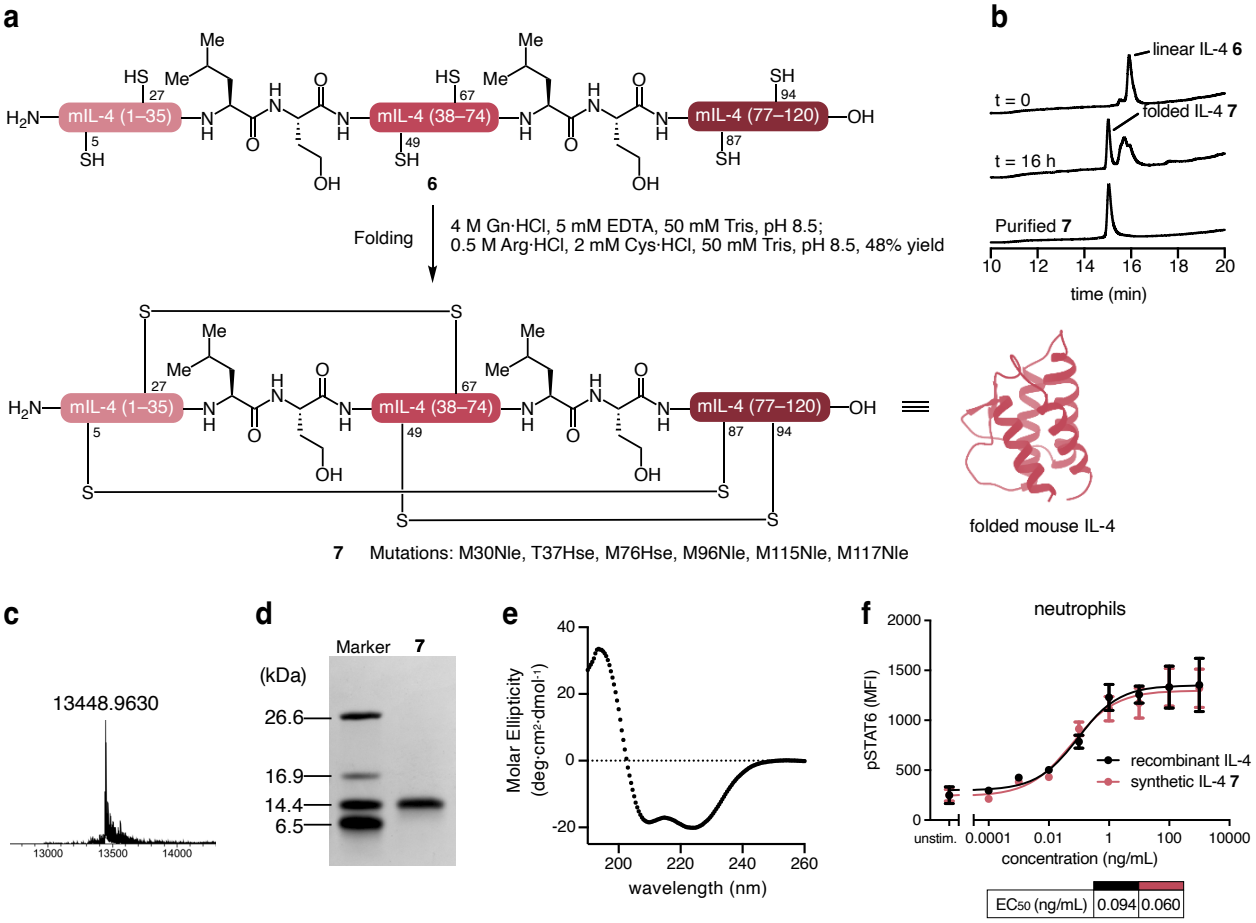

Fig. 3 a) Folding of synthetic IL-4. b) Analytical HPLC monitoring of folding. c) ESI-HRMS of folded smIL-4 **7**. d) SDS-PAGE of folded smIL-4 **7**. e) CD spectrum of folded smIL-4 **7**. f) Dose-dependent STAT6 phosphorylation by recombinant mIL-4 (rIL-4) and smIL-4 **7** in neutrophils.

To test the stimulatory activity of synthetic mouse IL-4 (smIL-4, **7**), smIL-4 was assessed for its ability to induce pSTAT6 and pSTAT5 in neutrophils, T and B cells from mouse spleen (Fig. 3f, Fig. S1, Fig. S2). In neutrophils, smIL-4 **7** successfully induced pSTAT6, reaching comparable EC50 values as rIL-4 (Fig. 3f). Taken together, the biological activity and characterization were consistent with successful synthesis and folding of smIL-4; the mutations (M30Nle, T37Hse, M76Hse, M96Nle, M115Nle, M117Nle) did not affect the biological activity.

Synthesis of IL-4Rα antagonist and activity-modulated IL-4 variants

With an effective synthesis of wild-type smIL-4 established, we adapted this synthetic route to the production of unique, defined mIL-4 variants. First, we aimed to synthesize smIL-4 that have modulated activity to the IL-4R complex by blocking the IL-4R signaling, a modality that could be potentially used to treat allergic disease. To engineer such a protein, we designed mutants and PEGylated smIL-4 constructs that should retain binding to the high-affinity IL-4Rα, but with attenuated or abrogated binding to the second receptor subunits γc or IL-13Rα1. Since the structure of mIL-4 has not been reported to date, the modification sites were selected to be Q116, based on the predicted structure generated by Swiss model (Fig. 4a), the human IL-4 (hIL-4) crystal structure complexed with receptors (PDB: 3BPO, 3 BPN), and sequence alignment of hIL-4 and mIL-4. Based on the synthetic route to wild-type smIL-4, five different variants **8-12** were synthesized and tested in vitro (Fig. 4c). The mutations Q116S (**8**) and Q116Orn (**9**) were chosen to test the effect of slight differences in the structure compared to Gln116. In addition,

the PEGylated variant smIL-4 Q116Orn(PEG-10 kDa) **11** was synthesized to block binding of the second receptor subunit using potassium acyltrifluoroborate (KAT) conjugation reaction[34,35] and the photoprotected intermediate before the ligation smIL-4 Q116Orn(photoHA) **10** was also tested in vitro. To assess the role of the site of PEGylation, variant S113Orn(PEG-10 kDa) **12** was prepared.

Since different STAT protein is associated with each receptor subunit and cells have different population of each receptor, both pSTAT5 and pSTAT6 signaling are expected in lymphocytes (T cells and B cells), and only pSTAT6 is expected in neutrophils when receptor complexes are formed with IL-4 variants, (Fig. 4b) whereas reduced pSTAT signaling is expected when the second receptor binding is hindered. smIL-4 Q116S mutant **8** had an overall loss of 50–70% pSTAT5 and pSTAT6 in T cells and neutrophils and did not show any cell type selectivity (Fig. 4d, Fig. S3). In contrast, IL-4 Q116Orn mutant **9** interestingly had significantly reduced activity in T cells, while maintaining comparable activity to rIL-4 in neutrophils (Fig. 4d, Fig. S3). This implied that the Q116S mutation biased IL-4 binding against γc without impacting binding to IL-13Rα1. When introducing a bulky small molecule at Q116, rather than a mutation (variant **10**), pSTAT was reduced in both T cells and neutrophils (Fig. 4e, Fig. S2). Introduction of an even bulkier PEG group (PEG-10 kDa) at Q116 (variant **11**) reduced pSTAT6 to the level seen with PBS in both T cells and neutrophils (Fig. 4f, Fig. S4). Intriguingly, when this PEG group was introduced at S113 (variant **12**), pSTAT6 was selectively affected in neutrophils, but not in T cells, resulting in the opposite effect of variant **9** (Fig. 4f, Fig. S4). An explanation for this difference could be that position S113 or its proximate environment is particularly important for the binding with IL-13Rα1, which is utilized for type II IL-4Rs in neutrophils, whereas Q116 and its surrounding environment is important for both the binding with γc and IL-13Rα1. Further investigation of smIL-4 Q116Orn(PEG-10 kDa) **11** by surface plasmon resonance (SPR) (Fig. S5) and in vitro competition assay against rIL-4 (Fig. S6) supported that this variant **11** could act as an antagonist.

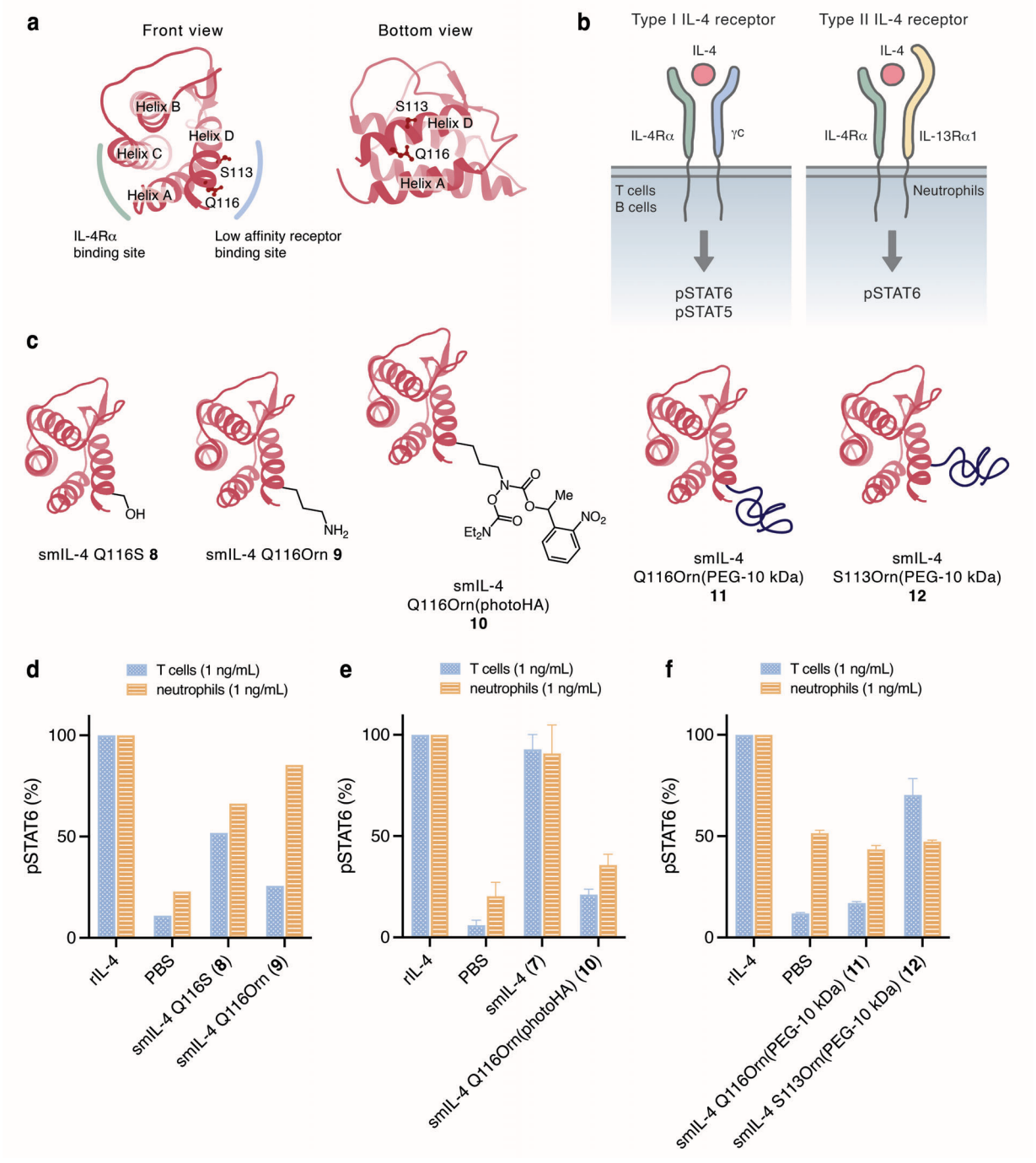

Fig. 4 a) The estimated structure of mouse IL-4 and chosen amino acid residues to introduce PEG groups located at receptor-binding sites. b) Scheme showing the IL-4 receptor signaling system and corresponding STAT proteins that are phosphorylated upon receptor engagement by cytokine. c) Synthesized and tested IL-4 variants. d-f) In vitro dose-dependent STAT6 phosphorylation by rIL-4, smIL-4 **7**, smIL-4 Q116S **8**, smIL-4 Q116Orn **9**, smIL-4 Q116Orn(photoHA) **10**, mIL-4 Q116Orn(PEG-10 kDa) **11**, mIL-4 S113Orn(PEG-10 kDa) **12** at 1 ng/mL concentration in T cells and neutrophils (For dose-dependent assay, see Fig. S2–4).

Design, synthesis and in vitro assessment of photocaged IL-4

The high potency and pleiotropic activities of cytokines can limit their therapeutic utility. To mitigate this, conditional activation strategies are in high demand and successful approaches include protease activation[36–38] and reducing potential- and pH-dependent exposure of cytokines.[39] The ability to chemically synthesize IL-4 opens new avenues for conditional activation, as caging groups that cannot be installed in recombinant cytokines can be easily introduced. As we observed that Q116 in mIL-4 is crucial for binding to the secondary low-affinity receptor subunit, we envisioned to synthesize smIL-4 with a photocleavable group at Q116, which could still bind to IL-4Rα; however, the second receptor subunit would not be recruited, abrogating the down-stream signaling until the photocaging group is removed by irradiation (Fig. 5a). Such an IL-4 variant could be of great interest to treat certain organ-specific autoimmune diseases, such as rheumatoid arthritis and psoriasis, by precisely controlling timing and location of activation without inducing systemic adverse side effects.

We embarked on photocaged IL-4 synthesis by designing and synthesizing photocaged glutamine **13** (Fig. 5b) as described in the Supporting Information, based on reported examples of photocaged amides.[40–42] Synthesized **13** was incorporated during SPPS and following our established modular synthetic route toward IL-4 provided us an IL-4 variant with photocaged glutamine at Q116 **14** (photoQ).

Folded, photocaged smIL-4 **14** was subjected to photo-uncaging tests (Fig. 5c). A solution of **14** in PBS was irradiated with 365 nm UV light. After 10 min of UV irradiation, the photocaging group was removed to reveal the native glutamine residue, as observed by RP-HPLC; the major peak corresponded to that of wild-type smIL-4 **7** (Fig. 5d) and exhibited the expected mass of smIL-4 **7** by HRMS.

The biological activity of photocaged smIL-4 **14** before and after UV decaging was tested by pSTAT assay (Fig. 5e). As expected, prior to UV irradiation **14** did not effectively induce signaling and failed to show any signaling activity in T cells, B cells, or neutrophils. After UV irradiation, however, the activity was completely restored to that of rIL-4. We attributed the small residual activity for STAT6 phosphorylation before UV irradiation to the small size of the photocaging group, which may not fully inhibit the formation of the receptor binding complex.

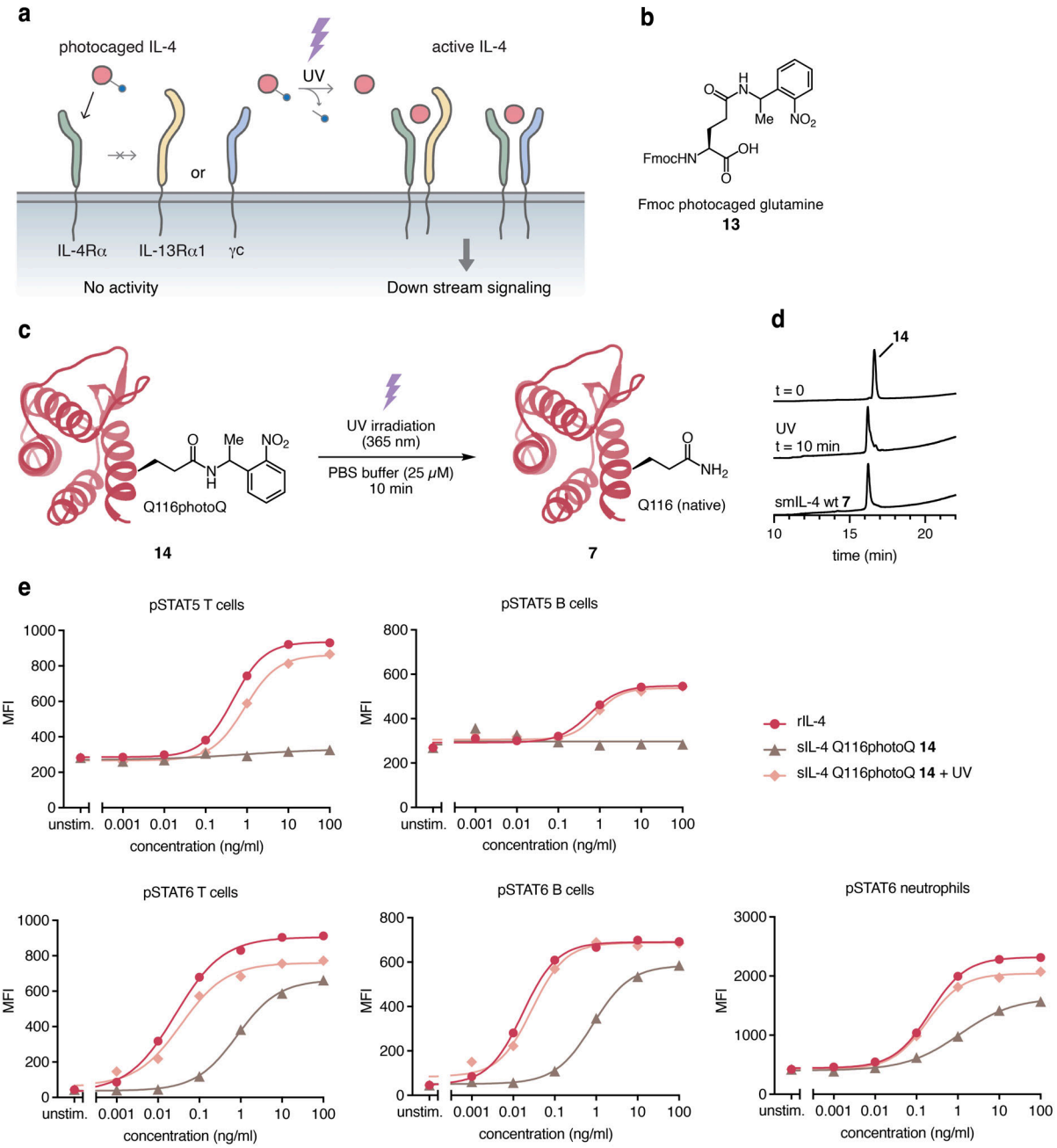

Fig. 5 a) Concept of photocaged IL-4. b) Photocaged glutamine as a Fmoc SPPS monomer. c-d) Deprotection of synthesized photocaged IL-4 and HPLC trace. e) Dose-dependent STAT phosphorylation by rIL-4 and photocaged IL-4 **14** with or without UV irradiation for 10 min in T cells, B cells, and neutrophils.

In vivo assessment of PEGylated photoQ IL-4

With these promising results *in vitro*, we proceeded with *in vivo* experiments in mice. Due to its small size, IL-4 has a short half-life *in vivo*. Half-life extension strategies include complexation of IL-4 with a particular anti-IL-4 monoclonal antibody (mAb), resulting in IL-4/anti-IL-4 mAb complexes[10], fusion to Fc fragments, or conjugation with half-life extending polymers. By using our flexible and modular chemical synthesis of IL-4, we prepared a PEGylated, photocaged IL-4. Introducing a PEG group is a well-established strategy to extend *in vivo* half-life of therapeutic proteins by increasing the molecular weight and hydrodynamic radius of the molecule.[43,44] To this end, an azidolysine was introduced at position N41, which is located in the loop between

helices A and B. This azidolysine was coupled with a dibenzocyclooctyne (DBCO) containing a PEG group via strain-promoted alkyne azide cycloaddition (SPAAC) to afford PEGylated photocaged smIL-4 **16** (Fig. 6a).[45,46] It should be noted that the previously employed KAT ligation was not employed in this particular case because the photoprotecting group of hydroxylamine amino acid is not orthogonal to photocaged glutamine **13**. The synthesis, folding, and characterization of the half-life-extended, photocaged smIL-4 **16** proceeded as expected.

The activity of PEGylated photocaged smIL-4 **16** was tested by inducing systemic neutrophilia by injection of recombinant mouse G-CSF and measuring whether blood counts of neutrophils were reduced by IL-4R engagement on neutrophils, as previously published.[10,47] We observed that PEGylated, photocaged smIL-4 **16** was unable to inhibit G-CSF-induced neutrophilia, as evidenced by neutrophil counts that were as high as in G-CSF-injected control mice treated with PBS. However, when the PEGylated photocaged IL-4 was treated with UV light prior to injection, neutrophil counts were suppressed, comparable to when using half-life-extended rIL-4/anti-IL-4 mAb complexes. This demonstrates that controlled activation of IL-4 using our photocage was successful. Moreover, PEGylation of photocaged IL-4 successfully extended the half-life of IL-4, and biological activity of IL-4 was seen *in vivo* without complexation to a mAb or another reagent. These data illustrate the potential of synthetic IL-4 variants to serve as conditionally activated cytokines.

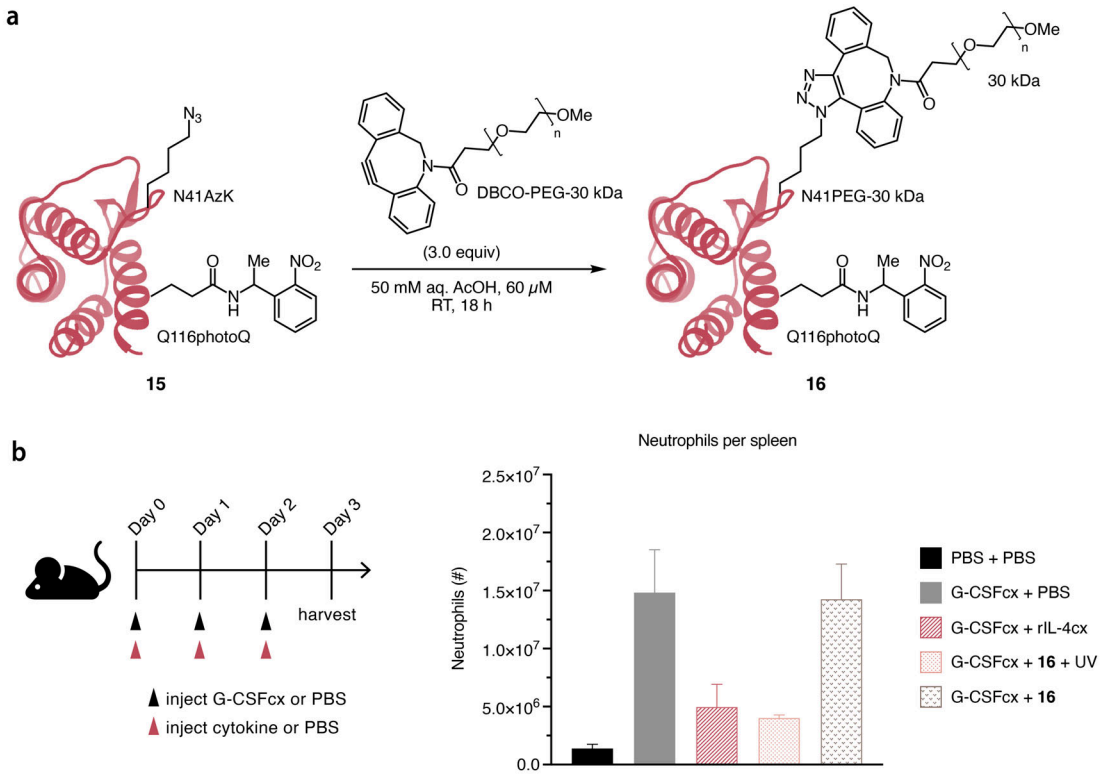

Fig. 6 a) PEGylation of photocaged IL-4 with azidolysine at N41 **15** using SPAAC reaction (only one regioisomer is shown). b) In vivo assay of photocaged IL-4 **16**. Mice were injected with half-life-extended G-CSF/anti-G-CSF mAb complexes (G-CSFcx, 1 μg/6 μg) and rIL-4/anti-IL-4 mAb complexes (rIL-4cx, 1.5 μg/15 μg) or PEGylated photocaged IL-4 **16** (5 μg) with or without UV irradiation for 10 min prior to injection. Mice were sacrificed on day 3 and neutrophil counts determined in spleen by flow cytometry.

Discussion

Cytokines are critical mediators of immune responses and they hold promise as next-generation therapies for various diseases. Their clinical use, however, is currently limited due to the lack of precise engineering methods to improve their short half-life and pleiotropism. Engineering of cytokines to modulate or emphasize the desired activity is essential to harness their therapeutic potential.

In this study, we have established a chemical synthesis of mIL-4 and demonstrated that this modular synthetic route can be utilized to produce two functionally different IL-4 variants: (i) activity modulated IL-4 variants that can block or differentiate between the two IL-4R types and (ii) photocaged IL-4 that acts as a spatiotemporally controlled agonist.

In addition to preparation of smIL-4 Q116Orn(PEG-10 kDa) **11**, an IL-4Rα antagonist with a PEG group at Q116 position, we found an important feature of some variants. The Q116Orn mutant **8** did not significantly affect the bioactivity in neutrophils, but this variant was not active in T cells. Contrarily, smIL-4 S113Orn(PEG-10 kDa) **12** selectively inhibited signaling only in neutrophils, while retaining activity in T cells. This information can be used to fine tune these residues and bias the binding to the two different secondary receptor subunits, with which they share the binding surface on mIL-4. Therefore, selective activation of one of these receptors is possible. These findings, which had not been previously observed by using recombinantly generated muteins of mIL-4, in principle enable the development of an antagonist variant of IL-4 selective to type II IL-4R.

In the second application of the chemical synthesis of mIL-4, we generated a multifunctional mIL-4 containing two unnatural amino acids. Q116, which proved to be an effective position to modulate binding to the secondary receptor subunit, was replaced with a photocaged glutamine residue which recovered its structure after UV irradiation. While half-life extension in blood circulation of photocaged smIL-4 was required to facilitate the biological activity *in vivo*, we successfully conjugated an additional PEG group to photocaged IL-4 by using SPAAC reaction for half-life extension, demonstrating the ease at which new types of multifunctional cytokines can be designed and engineered by using chemical protein synthesis.

For this proof-of-concept study of a photocaged IL-4 we prepared a photocaged Gln which required UV-A irradiation to remove the protecting group. While we could successfully demonstrate suppression of G-CSF-mediated neutrophil expansion in mice upon decaging the photocaged IL-4, use of this strategy is limited owing to the challenges associated with administering high-intensity UV-A light. The successful demonstration of this, however, lays the groundwork for alternative conditional activation approaches including photo-caging group at longer wavelengths or chemically induced uncaging.[48,49]

Collectively, chemical protein synthesis enabled us to access a variety of therapeutically valuable IL-4 variants that could not have been obtained otherwise. By establishing wild-type IL-4 synthesis as a platform, we could easily introduce almost any modifications at will to obtain differently functionalized proteins in combination with other organic chemistry methodologies. This concept can be extended to engineer other cytokines with selective functions for use as potential therapeutics.

Methods

Animals. C57BL/6 (referred to as B6) mice were purchased from Charles River Laboratories. Animal experiments were performed with 2 to 5 months old female mice in accordance with the Cantonal Veterinary Office of Zurich and with Swiss Federal and Cantonal Law.

Phosphorylated signal transducer and activator of transcription (STAT) signaling assay. Spleen isolated from C57BL/6 mice were processed into single cell suspension and resuspended in RPMI 1640 medium (Gibco) supplemented with 5% fetal bovine serum (FBS; Thermo

Fisher). The cells were left to rest for 1 h in an incubator (always at 37°C with 5% CO2). Hereafter, the bulk splenocytes were stimulated with varying concentrations of recombinant mouse nbvcxzIL-4 (rIL-4; PeproTech), synthetic IL-4, different variants of PEGylated IL-4s or IL-4 variants for 15 min in an incubator as indicated on the figures. For the competition assay, the PEGylated IL-4 variants were mixed with a fixed concentration of rIL-4 (1 ng/ml) prior to stimulation of cells. Afterwards, the cells were fix with Fix Buffer I (BD Phosflow) followed by permeabilization with Perm Buffer III (BD Phosflow) according to manufactures protocol. Phosphorylation of intracellular STATs was analyzed by flow cytometry.

Flow cytometry. Cells were stained for analysis by flow cytometry using fluorochrome-conjugated monoclonal antibodies directed against the following mouse antigens: CD3 (145-2C11; BD Biosciences), CD4 (GK1.5; eBioscience), CD11b (M1/70; BioLegend), CD19 (6D5; Biolegend), CD25 (7D4; eBioscience), CD44 (IM7; Biolegend), CD62L (MEL-14; BD Biosciences), CD124 (mIL4R-M1; BD Biosciences), CD132 (TUGm2; Biolegend), CD213a1 (13MOKA; Invitrogen), IgG2a (eBioscience), IgG2b (eBioscience), Ly6G (1A8; BioLegend), IL-4 (11B11; Invitrogen), IL-17A (eBio17B7; eBioscience), INFg (XMG1.2; eBioscience), MHC II (M5/114.15.2; eBioscience), pSTAT3 (Tyr705; 13A3-1; Biolegend), pSTAT5 (Tyr694; 47/Stat5(pY694); BD Phosflow), pSTAT6 (Tyr641; J71-773.58.11; BD Phosflow). Cells were acquired on a BD LSR Fortessa flow cytometer and analyzed using FlowJo software (Tristar).

Sterile inflammation model. B6 mice received intraperitoneal injections for three consecutive days of G-CSF/anti-G-CSF complexes (cx), made of 1 μg human G-CSF (Neupogen, Amgen) complexed with 6 μg anti-human G-CSF antibody (BVD11-37G10, SouthernBiotech) and for IL-4cx; 1.5 μg mouse IL-4 (PeproTech) complexed with 15 μg anti-IL-4 antibody (11B11, BioXcell) or indicated amount of uncomplexed cytokine. Mice were sacrificed 16 hours after the last injection and spleen, bone marrow and blood were processed into single-cell suspensions for analysis by flow cytometry. Cell surface staining of 2 $\times$ 106 cells was performed for 30 mins at 4°C with the following antibodies: BUV395–conjugated anti-CD11b (M1/70, BD Biosciences); BUV737–conjugated anti-CD3 (17A2, BD Biosciences); ef450–conjugated anti-Ly6C (HK1.4, Thermo Fisher); BV510–conjugated anti-CD19 (6D5, BioLegend); BV711–conjugated anti-NK1.1 (PK136, BioLegend); BV785–conjugated anti-CD11c (N418, BioLegend); FITC–conjugated anti-MHC II (M5/114.15.2, BioLegend); PE–conjugated anti-XCR1 (ZET, BioLegend); APC–conjugated anti-Ly6G (1A8, BioLegend) and Fixable Viability Dye eFluor™ 780 (Thermo Fisher). Samples were acquired on a BD LSR II flow cytometer (BD Biosciences) and analyzed using FlowJo software (BD Biosciences).

General procedures for Fmoc solid-phase peptide synthesis (SPPS). The following Fmoc-amino acids with side-chain protecting groups were used: Fmoc-Ala-OH, Fmoc-Arg(Pbf)-OH, Fmoc-Asn(Trt)-OH, Fmoc-Asp(OtBu)-OH, Fmoc-Cys(Acm)-OH, Fmoc-Gln(Trt)-OH, Fmoc-Glu(OtBu)-OH, Fmoc-Gly-OH, Fmoc-His(Trt)-OH, Fmoc-Ile-OH, Fmoc-Leu-OH, Fmoc-Lys(Boc)-OH, Fmoc-Nle-OH, Fmoc-Phe-OH, Fmoc-Pro-OH, Fmoc-Ser(tBu)-OH, Fmoc-Thr(tBu)-OH, Fmoc-Trp(Boc)-OH, Fmoc-Tyr(tBu)-OH, Fmoc-Val-OH.

Automated Fmoc SPPS. Peptides were synthesized on a CS Bio 136X synthesizer or on a Multisyntech Syro I parallel synthesizer or on a Symphony X multiple peptide synthesizer using Fmoc-SPPS chemistry. Fmoc deprotections were performed with 20% (v/v) piperidine in DMF (10 min x n) and washed with DMF (x 5). Unless stated, couplings were performed with Fmoc-Xaa-OH (4.0 equiv relative to resin loading), HCTU (3.95 equiv) and NMM (8.0 equiv) in DMF (45 min x 2) and washed with DMF (x 5). After coupling, unreacted free amine was capped by treatment with a mixture of acetic anhydride/NMM/DMF (1:1:4, v/v, 5 min x 2) and washed with DMF (x 5). Fmoc-Cys(Acm)-OH (4.0 equiv relative to resin loading) was coupled by using 6-Cl HOBt (4.0 equiv) and DIC (4.0 equiv) in DMF for 2h (x 1 unless stated). Pseudoprolines (2.0 equiv relative to resin loading) were coupled by using HATU (1.95 equiv) and NMM (4.0 equiv) for 2 h (x 1 unless stated).

Resin cleavage procedures. The dried resin was placed in a glass vial, the TFA cleavage cocktail (20 mL/g dried resin) was added and the suspension was shaken for 1.5–2 h. The resin was filtered and the volatiles were removed under reduced pressure. The residue was triturated with Et_2O (ca. 15 mL/g dried resin), centrifuged (3500 x g, 5 min) and the supernatant was removed by decantation. This trituration/washing step was repeated twice. The crude material was dried and dissolved in a suitable solvent (DMSO or H_2O/CH_3CN (1:1, v/v) containing 0.1% (v/v) TFA) for RP-HPLC purification. TFA cleavage cocktail compositions used: Cleavage cocktail A: TFA:DODT:H_2O (95:2.5:2.5, v/v/v), Cleavage cocktail B: TFA:TIPS:H_2O (95:2.5:2.5, v/v/v)

Synthesis of IL-4 wilde type 7.

Segment synthesis. H-[Cys(Acm)^{5,27}]-IL-4(1–35)-Leu-α-ketoacid **1** was synthesized on Rink-Amide polystyrene resin loaded with Fmoc-protected-Leu-α-ketoacid precursor (2.0 g, 0.22 mmol/g, 0.44 mmol). After automated Fmoc-SPPS up to His1, the peptide was cleaved from the resin using cleavage cocktail A. The resulting crude peptide was purified by preparative RP-HPLC using Shiseido Capcell Pak UG80 C18 column (5 µm, 80 Å pore size, 50 mm I.D. x 250 mm) at 60 °C with a gradient of 20 to 60% CH_3CN with 0.1% TFA over 30 min to obtain peptide segment **1** (313.4 mg, 18 %) as a white fluffy lyophilized powder. Opr-[Cys(Acm)^{49,67}]-IL-4(38–74)-photoprotected-Leu-α-ketoacid **2** was synthesized on Rink-Amide ChemMatrix loaded with Fmoc-photoprotected-Leu-α-ketoacid precursor (2.0 g, 0.24 mmol/g, 0.48 mmol). Pseudoproline Fmoc-Thr(tBu)-Thr(Ψ(Me,Me)pro)-OH and Fmoc-Ala-Ser(Ψ(Me,Me)pro)-OH were used at Thr42-Thr43 and Ala51-Ser52 (2 h x 2) and double couplings were applied for coupling of Fmoc-Cys(Acm)-OH at Cys49. After Fmoc-SPPS, the peptide was cleaved from the resin using cleavage cocktail A. The resulting crude peptide was purified by preparative RP-HPLC using Shiseido Capcell Pak UG80 C18 column (5 µm, 80 Å pore size, 50 mm I.D. x 250 mm) at 60 °C with a gradient of 20 to 50% CH_3CN with 0.1% TFA over 30 min to obtain peptide segment **2** (476 mg, 21 %) as a white fluffy lyophilized powder. Opr-[Cys(Acm)87,94]-IL-4(77–120)-OH **3** was synthesized on HMPB ChemMatrix resin loaded with Fmoc-Ser(tBu)-OH followed by Fmoc-Tyr(tBu)-OH (225 mg, 0.31 mmol/g, 70 mmol). Pseudoproline Fmoc-Ser-Thr(Ψ(Me,Me)pro)-OH was used at Ser101-Thr102 and double coupling was applied for coupling of BocOpr at the end. After Fmoc-SPPS, the

peptide was cleaved from the resin using cleavage cocktail B. The resulting crude peptide was purified by preparative RP-HPLC using Shiseido Capcell Pak UG80 C18 column (5 µm, 80 Å pore size, 50 mm I.D. x 250 mm) at 60 °C with a gradient of 20 to 70% CH_3CN with 0.1% TFA over 40 min to obtain peptide segment **3** (12.2 mg, 3.3 %) as a white fluffy lyophilized powder.

Ligations. Segment **1** (113 mg, 27.4 mmol, 1.3 equiv) and segment **2** (100 mg, 21.1 mmol, 1.0 equiv) were dissolved in 9:1 DMSO:H_2O with 0.1 M oxalic acid (1.05 mL, 20 mM). After stirring for 15 h at 60 °C, the mixture was cooled to room temperature, diluted with 1:1 CH_3CN:H_2O with 0.1% TFA (7.0 mL, 3 mM) and irradiated at a wavelength of 365 nm for 45 min at room temperature. This reaction mixture was purified by preparative RP-HPLC using Shiseido Capcell Pak UG80 C18 column (50 x 250 mm) at 60 °C with a gradient of 20 to 60% CH_3CN with 0.1% TFA over 28 min to obtain peptide **4** (91.7 mg, 51 %) as a fluffy lyophilized powder. Polypeptide **4** (25.0 mg, 2.91 mmol, 1.0 equiv) and segment **3** (20.1 mg, 3.78 mmol, 1.3 equiv) were dissolved in 9:1 DMSO:H_2O with 0.1 M oxalic acid (146 mL, 20 mM). After stirring for 24 h at 60 °C, the resulting gel-like mixture was dissolved with DMSO (400 mL) then added a buffer containing 50 mM sodium carbonate and 6 M Gn·HCl pH 9.5 (1.5 mL, 2 mM). After incubating for 2.5 h, the mixture was acidified by adding 50% aq. AcOH and purified by preparative RP-HPLC using Shiseido Capcell Pak MGII C18 column (5 µm, 120 Å pore size, 20 mm I.D. x 250 mm) at 60 °C with a gradient of 20 to 70% CH_3CN with 0.1% TFA over 28 min to obtain **5** (13.4 mg, 33% over 2 steps as a white fluffy lyophilized powder.

Acm deprotection. Polypeptide **5** (13.4 mg, 965 nmol) was dissolved in 50% aq. AcOH and AgOAc (32.0 mg, 191 mmol, 200 equiv) was added. After shaking at 50 °C for 2 h in the dark, the mixture was cooled to room temperature and DTT (32.0 mg, 207 mmol, 215 equiv) was added. The formed precipitate was separated after centrifugation and the precipitate was washed twice with 50% aq. AcOH. The combined supernatant was purified by preparative RP-HPLC using Shiseido Capcell Pak MGII C18 column (5 µm, 120 Å pore size, 20 mm I.D. x 250 mm) at 60 °C with a gradient of 30 to 85% CH_3CN with 0.1% TFA over 28 min to obtain **6** (10.2 mg, 79%) as a fluffy lyophilized powder.

Folding. Polypeptide **6** (1.0 mg, 74.3 nmol, 1.0 equiv) was dissolved in solubilizing buffer 2.0 mL (0.5 mg/mL) containing 4 M Gn·HCl, 50 mM tris and 5 mM EDTA (pH 8.5). This solution was diluted 6-fold with 4 mL of folding buffer containing 0.5 M Arg·HCl, 50 mM tris, 2 mM Cys (pH 8.5) and incubated 18 h at room temperature. The mixture was acidified with 50% aq. AcOH and purified by preparative RP-HPLC using Shiseido Proteonavi column (5 µm, 300 Å pore size, 10 mm I.D. x 250 mm) at room temperature with a gradient of 20 to 75% CH_3CN with 0.1% TFA over 28 min to obtain folded wild type IL-4 **7** (483 mg, 48%, calculated based on the UV absorbance at 280 nm in H_2O).

Material availability. Materials that are not available commercially can be requested from the corresponding authors.

Data availability

Data are available within the Article, Supplementary Information or available from the authors upon request.

References

1. Zheng, X., Wu, Y., Bi, J., Huang, Y., Cheng, Y., Li, Y., Wu, Y., Cao, G. & Tian, Z. The use of supercytokines, immunocytokines, engager cytokines, and other synthetic cytokines in immunotherapy. *Cell Mol. Immunol.* **19,** 192–209 (2022).

2. Holder, P. G., Lim, S. A., Huang, C. S., Sharma, P., Dagdas, Y. S., Bulutoglu, B. & Sockolosky, J. T. Engineering interferons and interleukins for cancer immunotherapy. *Adv. Drug Deliv. Rev.* **182,** 114112 (2022).

3. Levin, A. M., Bates, D. L., Ring, A. M., Krieg, C., Lin, J. T., Su, L., Moraga, I., Raeber, M. E., Bowman, G. R., Novick, P., Pande, V. S., Fathman, C. G., Boyman, O. & Garcia, K. C. Exploiting a natural conformational switch to engineer an interleukin-2 'superkine.' *Nature* **484,** 529–533 (2012).

4. Junttila, I. S., Creusot, R. J., Moraga, I., Bates, D. L., Wong, M. T., Alonso, M. N., Suhoski, M. M., Lupardus, P., Meier-Schellersheim, M., Engleman, E. G., Utz, P. J., Fathman, G. C., Paul, W. E. & Garcia, C. K. Redirecting cell-type specific cytokine responses with engineered interleukin-4 superkines. *Nat. Chem. Biol.* **8,** 990–998 (2012).

5. Silva, D.-A., Yu, S., Ulge, U. Y., Spangler, J. B., Jude, K. M., Labão-Almeida, C., Ali, L. R., Quijano-Rubio, A., Ruterbusch, M., Leung, I., Biary, T., Crowley, S. J., Marcos, E., Walkey, C. D., Weitzner, B. D., Pardo-Avila, F., Castellanos, J., Carter, L., Stewart, L., Riddell, S. R., Pepper, M., Bernardes, G. J. L., Dougan, M., Garcia, K. C. & Baker, D. De novo design of potent and selective mimics of IL-2 and IL-15. *Nature* **565,** 186–191 (2019).

6. Sockolosky, J. T., Trotta, E., Parisi, G., Picton, L., Su, L. L., Le, A. C., Chhabra, A., Silveria, S. L., George, B. M., King, I. C., Tiffany, M. R., Jude, K., Sibener, L. V., Baker, D., Shizuru, J. A., Ribas, A., Bluestone, J. A. & Garcia, K. C. Selective targeting of engineered T cells using orthogonal IL-2 cytokine-receptor complexes. *Science* **359,** 1037–1042 (2018).

7. LaPorte, S. L., Juo, S. Z., Vaclavikova, J., Colf, L. A., Qi, X., Heller, N. M., Keegan, A. D. & Garcia, C. K. Molecular and structural basis of cytokine receptor pleiotropy in the interleukin-4/13 system. *Cell* **132,** 259–272 (2008).

8. Akaiwa, M., Yu, B., Umeshita-Suyama, R., Terada, N., Suto, H., Koga, T., Arima, K., Matsushita, S., Saito, H., Ogawa, H., Furue, M., Hamasaki, N., Ohshima, K. & Izuhara, K. Localization of human interleukin 13 receptor in non-haematopooetic cells. *Cytokine* **13,** 75–84 (2001).

9. Junttila, I. S. Tuning the cytokine responses: An update on interleukin (IL)-4 and IL-13 receptor complexes. *Front. immunol.* **9,** 888 (2018).

10. Woytschak, J., Keller, N., Krieg, C., Impellizzieri, D., Thompson, R. W., Wynn, T. A., Zinkernagel, A. S. & Boyman, O. Type 2 interleukin-4 receptor signaling in neutrophils antagonizes their expansion and migration during infection and inflammation. *Immunity* **45,** 172–184 (2016).

11. Nelms, K., Keegan, A. D., Zamorano, J., Ryan, J. J. & Paul, W. E. The IL-4 receptor: Signaling mechanisms and biologic functions. *Annu. Rev. Immunol.* **17,** 701–738 (1999).

12. Impellizzieri, D., Ridder, F., Raeber, M. E., Egholm, C., Woytschak, J., Kolios, A. G. A., Legler, D. F. & Boyman, O. Interleukin-4 receptor engagement in human neutrophils impairs their migration and extracellular trap formation. *J. Allergy Clin. Immunol.* **144,** 267–179.e2 (2019).

13. Akdis, C. A., Arkwright, P. D., Brüggen, M.-C., Busse, W., Gadina, M., Guttman-Yassky, E., Kabashima, K., Mitamura, Y., Vian, L., Wu, J. & Palomares, O. Type 2 immunity in the skin and lungs. *Allergy* **75,** 1582–1605 (2020).

14. Kruse, N., Shen, B. J., Arnold, S., Tony, H. P., Müller, T. & Sebald, W. Two distinct functional sites of human interleukin 4 are identified by variants impaired in either receptor binding or receptor activation. *EMBO J.* **12,** 5121–5129 (1993).

15. Andrews, A.-L., Holloway, J. W., Holgate, S. T. & Davies, D. E. IL-4 receptor α is an important modulator of IL-4 and IL-13 receptor binding: implications for the development of therapeutic targets. *J. Immunol.* **176,** 7456–7461 (2006).

16. Duppatla, V., Gjorgjevikj, M., Schmitz, W., Hermanns, H. M., Schäfer, C. M., Kottmair, M., Müller, T. & Sebald, W. IL-4 analogues with site-specific chemical modification at position 121 inhibit IL-4 and IL-13 biological activities. *Bioconjugate Chem.* **25,** 52–62 (2014).

17. Rathinam, K. K., Abraham, J. J. & Vijayakumar, T. M. An evidence based review of Dupilumab in the treatment of moderate to severe asthma. *Curr. Ther. Res.* **91,** 45–51 (2019).

18. Din, A. T. U., Malik, I., Arshad, D. & Din, A. T. U. Dupilumab for atopic dermatitis: The silver bullet we have been searching for? *Cureus* **12,** e7565 (2020).

19. Gooderham, M. J., Hong, H. C., Eshtiaghi, P. & Papp, K. A. Dupilumab: A review of its use in the treatment of atopic dermatitis. *J. Am. Acad. Dermatol.* **78,** S28–S36 (2018).

20. Chiang, C.-C., Cheng, W.-J., Korinek, M., Lin, C.-Y. & Hwang, T.-L. Neutrophils in psoriasis. *Front. Immunol.* **10,** 2376 (2019).

21. Wang, W.-M. & Jin, H.-Z. Role of neutrophils in psoriasis. *J. Immunol. Res.* **2020,** 1–6 (2020).

22. Grigolato, F., Egholm, C., Impellizzieri, D., Arosio, P. & Boyman, O. Establishment of a scalable microfluidic assay for characterization of population-based neutrophil chemotaxis. *Allergy* **75,** 1382–1393 (2020).

23. Impellizzieri, D., Egholm, C., Valaperti, A., Distler, O. & Boyman, O. Patients with systemic sclerosis show phenotypic and functional defects in neutrophils. *Allergy* **77,** 1274–1284 (2022).

24. Egholm, C., Özcan, A., Breu, D. & Boyman, O. Type 2 immune predisposition results in accelerated neutrophil aging causing susceptibility to bacterial infection. *Sci. Immunol.* **7,** eabi9733 (2022).

25. Martin, R. Interleukin 4 treatment of psoriasis: are pleiotropic cytokines suitable therapies for autoimmune diseases? *Trends Pharmacol. Sci.* **24,** 613–616 (2003).

26. Ghoreschi, K., Thomas, P., Breit, S., Dugas, M., Mailhammer, R., Eden, W. van, Zee, R. van der, Biedermann, T., Prinz, J., Mack, M., Mrowietz, U., Christophers, E., Schlöndorff, D., Plewig, G., Sander, C. A. & Röcken, M. Interleukin-4 therapy of psoriasis induces Th2 responses and improves human autoimmune disease. *Nat. Med.* **9,** 40–46 (2003).

27. Bode, J. W. Chemical protein synthesis with the α-ketoacid–hydroxylamine ligation. *Acc. Chem. Res.* **50,** 2104–2115 (2017).

28. Murar, C. E., Ninomiya, M., Shimura, S., Karakus, U., Boyman, O. & Bode, J. W. Chemical synthesis of interleukin-2 and disulfide stabilizing analogues. *Angew. Chem. Int. Ed.* **59,** 8425–8429 (2020).

29. Mueller, T. D., Zhang, J.-L., Sebald, W. & Duschl, A. Structure, binding, and antagonists in the IL-4/IL-13 receptor system. *Biochim. Biophys. Acta Mol. Cell Res.* **1592,** 237–250 (2001).

30. Carr, C., Aykent, S., Kimack, N. & Levine, A. Disulfide assignments in recombinant mouse and human interleukin 4. *Biochemistry* **30,** 1515–1523 (1991).

31. Kruse, N., Lehrnbecher, T. & Sebald, W. Site-directed mutagenesis reveals the importance of disulfide bridges and aromatic residues for structure and proliferative activity of human Interleukin-4. *FEBS Lett.* **286,** 58–60 (1991).

32. Durek, T., Torbeev, V. Yu. & Kent, S. B. H. Convergent chemical synthesis and high-resolution x-ray structure of human lysozyme. *Proc. Natl. Acad. Sci. U.S.A.* **104,** 4846–4851 (2007).

33. Wöhr, T., Wahl, F., Nefzi, A., Rohwedder, B., Sato, T., Sun, X. & Mutter, M. Pseudo-prolines as a solubilizing, structure-disrupting protection technique in peptide synthesis. *J. Am. Chem. Soc.* **118,** 9218–9227 (1996).

34. White, C. J. & Bode, J. W. PEGylation and dimerization of expressed proteins under near equimolar conditions with potassium 2-pyridyl acyltrifluoroborates. *ACS Cent. Sci.* **4,** 197–206 (2018).

35. Boross, G. N., Schauenburg, D. & Bode, J. W. Chemoselective derivatization of folded synthetic insulin variants with potassium acyltrifluoroborates (KATs). *Helv. Chim. Acta* **102,** e1800214 (2019).

36. Hsu, E. J., Cao, X., Moon, B., Bae, J., Sun, Z., Liu, Z. & Fu, Y.-X. A cytokine receptor-masked IL2 prodrug selectively activates tumor-infiltrating lymphocytes for potent antitumor therapy. *Nat. Commun.* **12,** 2768 (2021).

37. Cao, X., Liang, Y., Hu, Z., Li, H., Yang, J., Hsu, E. J., Zhu, J., Zhou, J. & Fu, Y.-X. Next generation of tumor-activating type I IFN enhances anti-tumor immune responses to overcome therapy resistance. *Nat. Commun.* **12,** 5866 (2021).

38. Guo, J., Liang, Y., Xue, D., Shen, J., Cai, Y., Zhu, J., Fu, Y.-X. & Peng, H. Tumor-conditional IL-15 pro-cytokine reactivates anti-tumor immunity with limited toxicity. *Cell Res.* **31,** 1190–1198 (2021).

39. Zhao, Y., Xie, Y.-Q., Herck, S. V., Nassiri, S., Gao, M., Guo, Y. & Tang, L. Switchable immune modulator for tumor-specific activation of anticancer immunity. *Sci. Adv.* **7,** eabg7291 (2021).

40. Ramesh, D., Wieboldt, R., Billington, A. P., Carpenter, B. K. & Hess, G. P. Photolabile precursors of biological amides: synthesis and characterization of caged o-nitrobenzyl derivatives of glutamine, asparagine, glycinamide, and .gamma.-aminobutyramide. *J. Org. Chem.* **58,** 4599–4605 (1993).

41. Awad, L., Jejelava, N., Burai, R. & Lashuel, H. A. A new caged-glutamine derivative as a tool to control the assembly of glutamine-containing amyloidogenic peptides. *ChemBioChem* **17,** 2353–2360 (2016).

42. Moulton, K. R., Sadiki, A., Koleva, B. N., Ombelets, L. J., Tran, T. H., Liu, S., Wang, B., Chen, H., Micheloni, E., Beuning, P. J., O'Doherty, G. A. & Zhou, Z. S. Site-specific reversible protein and peptide modification: Transglutaminase-catalyzed glutamine conjugation and bioorthogonal light-mediated removal. *Bioconjugate Chem.* **30,** 1617–1621 (2019).

43. Alconcel, S. N. S., Baas, A. S. & Maynard, H. D. FDA-approved poly(ethylene glycol)– protein conjugate drugs. *Polym. Chem.* **2,** 1442–1448 (2011).

44. Belén, L. H., Rangel-Yagui, C. de O., Lissabet, J. F. B., Effer, B., Lee-Estevez, M., Pessoa, A., Castillo, R. L. & Farías, J. G. From synthesis to characterization of site-selective PEGylated proteins. *Front. Pharmacol.* **10,** 1450 (2019).

45. Debets, M. F., Berkel, S. S. van, Schoffelen, S., Rutjes, F. P. J. T., Hest, J. C. M. van & Delft, F. L. van. Aza-dibenzocyclooctynes for fast and efficient enzyme PEGylation via copper-free (3+2) cycloaddition. *Chem. Commun.* **46,** 97–99 (2009).

46. Zhang, B., Xu, H., Chen, J., Zheng, Y., Wu, Y., Si, L., Wu, L., Zhang, C., Xia, G., Zhang, L. & Zhou, D. Development of next generation of therapeutic IFN-α2b via genetic code expansion. *Acta Biomater.* **19,** 100–111 (2015).

47. Semerad, C. L., Liu, F., Gregory, A. D., Stumpf, K. & Link, D. C. G-CSF is an essential regulator of neutrophil trafficking from the bone marrow to the blood. *Immunity* **17,** 413–423 (2002).

48. Pirrung, M. C., Pieper, W. H., Kaliappan, K. P. & Dhananjeyan, M. R. Combinatorial discovery of two-photon photoremovable protecting groups. *Proc. Natl. Acad. Sci. U.S.A.* **100,** 12548–12553 (2003).

49. Hansen, M. J., Velema, W. A., Lerch, M. M., Szymanski, W. & Feringa, B. L. Wavelength-selective cleavage of photoprotecting groups: strategies and applications in dynamic systems. *Chem. Soc. Rev.* **44,** 3358–3377 (2015).

Acknowledgements

Christopher J. White provided the PEG-potassium 2-pyridyl acyltrifluoroborates. The Molecular and Biomolecular Analysis Service (MoBiAS) of the Department of Chemistry and Applied Biosciences at ETH Zürich provided mass spectrometery. This work was supported by the ETH Zürich, the University of Zurich, the Swiss government excellence scholarship, and the Swiss National Science Foundation (grants no. 189950 and 310030-200669).

Author contributions

M.N. designed and performed experiments, analyzed the data, and wrote the manuscript. C.E. designed and performed experiments, analyzed the data, and revised the manuscript. D.B. designed and performed experiments, and analyzed the data. J.B and O.B. supervised the project, designed experiments, analyzed the data, and revised the manuscript.

Competing interests

The authors declare that they have no competing interests.